

EFFECT OF CALCINATION ON THE SINTERING BEHAVIOUR OF HYDROXYAPATITE

Y. C. TEH*, #C. Y. TAN*, S. RAMESH*, J. PURBOLAKSONO*, Y. M. TAN*,
HARI CHANDRAN**, W.D. TENG***, B.K. YAP****

*Centre for Advance Manufacturing & Materials Processing, Department of Mechanical Engineering, Faculty of Engineering, University of Malaya 50603, Kuala Lumpur, Malaysia

**Division of Neurosurgery, Faculty of Medicine, University of Malaya, Kuala Lumpur 50603, Malaysia

***Ceramics Technology Group, SIRIM Berhad, Shah Alam 40911, Malaysia

****Department of Electronics and Communication, College of Engineering, Universiti Tenaga Nasional, Km-7, Jalan Ikram-UNITEN, 43009 Kajang, Selangor, Malaysia

#E-mail: chouyong@um.edu.my

Submitted November 20, 2014; accepted December 29, 2014

Keywords: Hydroxyapatite, Calcination, Powder Morphology, Sintering

In this study, a wet chemically produced hydroxyapatite (HA) powder was subjected to calcination at 700, 800, 900 and 1000°C. Subsequently, the sintering behaviour of these calcined powders was studied at various temperatures, ranging from 1050 to 1350°C. XRD results revealed that calcination has no effect on the phase stability of hydroxyapatite. However, the XRD peaks showed that the crystallinity of the powder increased with increasing calcination temperature. The specific surface area of powder reduced drastically from 60.74 m²·g⁻¹ to 9.45 m²·g⁻¹ with increasing calcination temperature. The SEM micrographs of calcined powder showed the coarsening of powder particles as the calcination temperature was increased. In terms of sinterability, the uncalcined HA powder sintered at 1150°C was found to possess the optimum properties with the following values being recorded: ~ 99 % relative density, Vickers hardness of 7.23 GPa and fracture toughness of 1.12 MPa·m^{1/2}. The present research indicated that calcination of the HA powder prior to sintering has a negligible effect on the sintering behaviour of the HA compacts and that calcination at 1000°C was found to be unfavourable to the properties of sintered HA.

INTRODUCTION

Back in the yester years, bone transplants were the most popular method to replace damaged hard tissue or bones. However, as more transplantations were done, it was realized that this method could be hazardous to the patient because of the risk of disease transmission and adverse immune reactions, not to mention the scarcity of donors [1]. Therefore, transplantation was being replaced by implantation wherever possible. As a result, the demand for artificial implant materials has increased risen and research has been directed towards bioceramics as they are biocompatible with the human body, easy to process and some of its properties are similar to hard tissues [2, 3].

Over the years, continuous research has led to the development of hydroxyapatite (HA) as the most suitable bioceramic for use as a bone implant due to its chemical resemblance to bone mineral [4]. The uniqueness of HA is that strong bonds can be formed between the human bone and hydroxyapatite with no fibrous tissue encapsulating the implant's interface [4]. Hence, HA found its way into

the world of clinical applications, including applications as dental implants and for periodontal treatment [5]. The only drawback of HA is its low fracture toughness which limits its use in load-bearing clinical applications. This led to further research and the development to produce HA with improved mechanical properties, while still retaining the biocompatibility of the ceramic [6, 7].

It has been found by other researchers [8-13] that different methods of synthesizing HA affect the sinterability and mechanical properties of the resulting sintered body. Nevertheless, in all these works, the wet chemical precipitation method was preferred as it is a versatile low-cost method [14]. It was also reported that calcination of the HA powders upon synthesizing could affect the morphology of the particles [15] and increase the degree of crystallinity of the particles [16]. Nevertheless, the effect of calcination on the sintering properties of the calcined powders is known to be limited. Thus, the primary objective of this work is to investigate the sintering behaviour of synthesized HA powder after calcination at 700, 800, 900 and 1000°C.

EXPERIMENTAL

Materials and Methods

Preparation of hydroxyapatite powder via wet precipitation method

In the current work, the HA powder used was prepared according to a wet chemical method consisting in the precipitation from an aqueous medium by the slow addition of orthophosphoric acid (H_3PO_4) solution to a calcium hydroxide ($Ca(OH)_2$) [17]. The synthesized HA powder was calcined in air atmosphere at temperatures ranging from 700°C to 1000°C at a rate of 10°C·min⁻¹ and, after a dwell time of 2 hours, cooled to room temperature at a rate of 10°C·min⁻¹.

Green body preparation

Upon completing the formation of hydroxyapatite, the powder was uniaxially pressed at 2.5 MPa pressure to form a disc. Cold isostatic pressing at 200 MPa was applied to the green samples followed by pressureless sintering in air using a rapid heating furnace over the temperature range of 1050 - 1350°C. The ramp rate was 2°C·min⁻¹ (heating and cooling) and soaking time of 2 hours for each firing. All sintered samples were then polished to a 1 µm surface finish prior to characterization.

Characterization of hydroxyapatite powder and ceramics

The calcium and phosphorus content in the synthesized HA powder were determined by using the Inductively Coupled Plasma-Atomic Emission Spectrometry (ICP-AES) technique. The particle size distributions of the HA powders were determined using a SediGraph 5100 X-ray particle size analyzer (Micromeritics, USA). The specific surface area of the powder was measured by the Brunauer-Emmett-Teller (BET) method. The morphology of the starting powder was examined using a Philips SEM model XL30 scanning electron microscope (SEM). Phase analysis of both powders and sintered samples was analysed using X-ray diffraction (XRD -, Rigaku Geiger-Flex, Japan). A Fourier transform infrared spectrometer (FTIR - Bruker IFS-66-VS, Germany) with a reflectance mode was used for qualitative analysis of the molecular radicals. Prior to testing, 40 mg of KBr was mixed with 0.4 mg of the tested powder. Subsequently, the powder was pressed into pellet with diameter 13 mm. Possible structural variations and reactions in the samples were

examined. Infrared spectra with a resolution of 4 cm⁻¹ and a scan number of 32 were recorded with a scan range of 400 - 4000 cm⁻¹. After sintering, the bulk densities of the sintered compacts were determined by the water immersion technique (Mettler Toledo, Switzerland). The relative density was calculated by taking the theoretical density of HA as 3.156 g·cm⁻³. The microhardness (Hv) of the samples was determined using the Vickers indentation method (Matsuzawa, Japan). The indentation fracture toughness (K_{Ic}) was determined from the equation derived by Niihara et al. [18].

RESULTS AND DISCUSSION

The results of chemical analysis, particle size analysis and specific surface area (SSA) measurement carried out on the calcined and uncalcined HA powders are shown in Table 1. All the HA powders exhibited a value of 1.667 for the Ca/P ratio, indicating that the calcination had negligible effect on the Ca/P ratio. Particle size analysis of the calcined HA powders revealed that the mean particle size increased from 1.78 ± 0.22 µm for uncalcined HA to 2.25 ± 0.68 µm when calcined at 1000°C as shown in Table 1. This observation correlated well with the trend observed by Juang and Hon [19] who found that the mean particle size increased from 0.97 µm for uncalcined HA to 4.19 µm for HA powder calcined at 1000°C.

The specific surface area (SSA) of the powders as listed in Table 1 shows that the uncalcined HA has the largest SSA (60.74 m² g⁻¹) of all the powders prepared. Increasing the calcination temperature from 700°C to 1000°C resulted in an almost linear decrease in the SSA, which correlated well with the increasing particle size. This finding is in agreement with the studies reported by Senamaud et al. [20]. These authors suggested that the surface area reduction of the powders during calcination should be attributed to particle coalescence with increasing temperature.

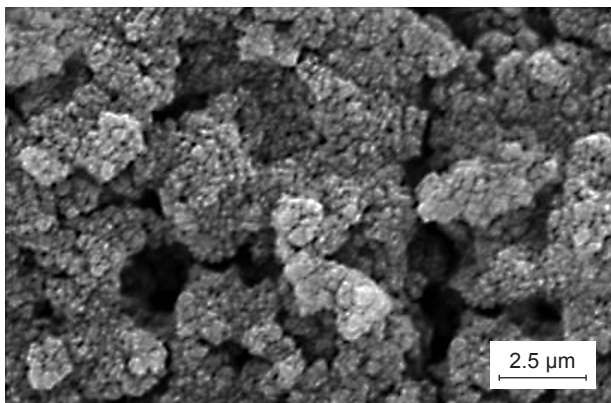
The morphologies of the uncalcined and calcined HA powders are shown in Figure 1a-e. The observed particle sizes increased slightly for a calcination temperature of 700°C (Figure 1b) when compared to uncalcined HA powder (Figure 1a), and this correlated well with the particle size analysis results shown in Table 1. For uncalcined powder and powder calcined at low temperature (700°C), the surface appeared to be composed of very tiny particles.

Table 1. Properties of the HA powders at different calcination temperatures.

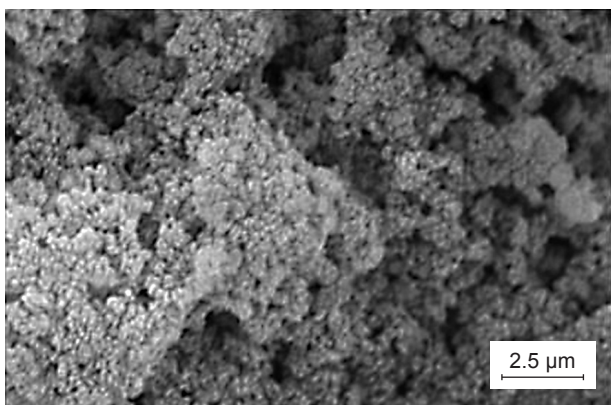
	Uncalcined HA	Calcined HA @ 700°C	Calcined HA @ 800°C	Calcined HA @ 900°C	Calcined HA @ 1000°C
Colour	white	white	white	white	white
Ca/P ratio	1.667	1.667	1.667	1.667	1.667
Mean particle size (µm)	1.78 ± 0.22	1.87 ± 0.45	2.04 ± 0.06	2.14 ± 0.23	2.25 ± 0.68
Specific surface area/SSA (m ² ·g ⁻¹)	60.74	20.7	15.16	9.49	9.45

As the calcination temperature increased from 700 to 800°C, the tiny particles coalesce to form larger particles as illustrated in Figure 1c. This coalescence is associated with the initial stage of sintering. At higher temperatures, the powder particles appeared to have fused together forming larger agglomerates and a coarser microstructure. A change in the surface morphology of powders was observed when the calcination temperature increased from 900 to 1000°C, where neck formation bridging neighbouring particles was observed as illustrated in Figure 1d and Figure 1e. It can be concluded that calcination has a significant effect on the particle morphology and properties. The significant decrease in specific surface area stated in Table 1 could be associated to the agglomeration and coarsening of particles as the calcination was increased, as depicted in the SEM micrographs.

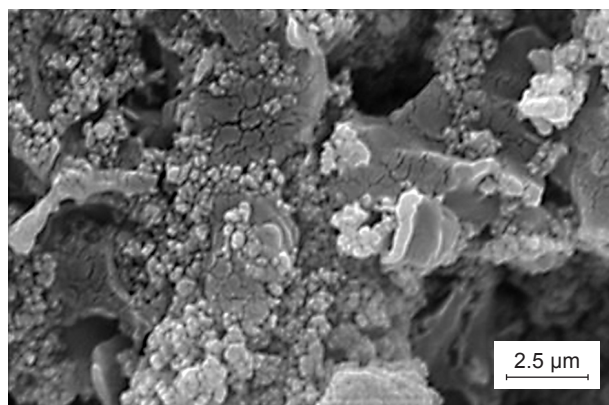
The X-ray diffractograms of the calcined powders in Figure 2 show that calcination does not affect the phase composition. There was no secondary phase detected, a fact that is in agreement with the observations made by other researchers [15, 19]. Although calcination has no effect on the HA phase stability, it was found that the crystallinity of the powders is highly affected by the calcination temperature. For uncalcined powder and powder calcined at 700°C, broad diffraction peaks were observed as shown in Figure 2. However, there was a clear change in the height and width of the diffraction peaks when the calcination temperature increased beyond 700°C. The XRD peaks for powders calcined at 800, 900 and 1000°C were sharper due to well crystallized phase. This observation showed that increasing the calcination temperature resulted in higher crystallinity of the powders.



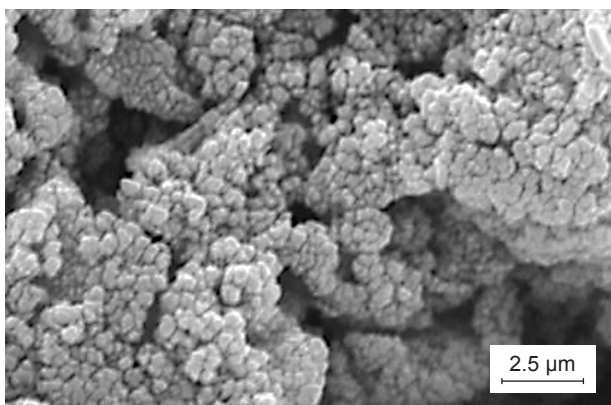
a) uncalcined



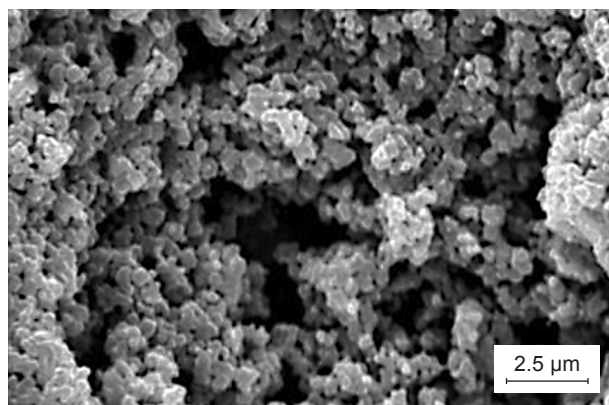
b) calcined at 700°C



d) calcined at 900°C



c) calcined at 800°C



e) calcined at 1000°C

Figure 1. SEM micrographs of HA powders: a) uncalcined; b) calcined at 700°C; c) calcined at 800°C; d) calcined at 900°C; e) calcined at 1000°C.

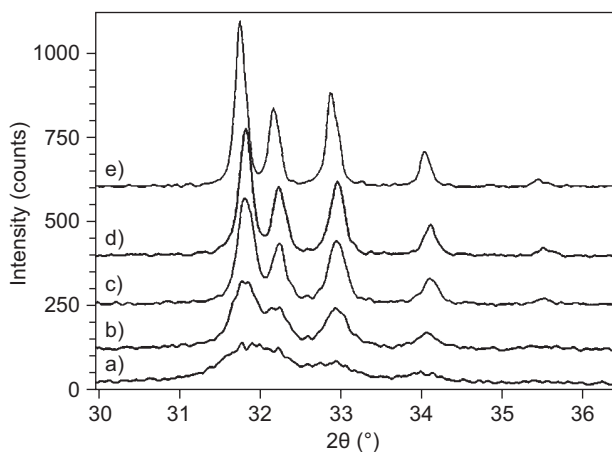


Figure 2. Comparison of XRD traces of HA powders: a) uncalcined; b) calcined at 700°C; c) calcined at 800°C; d) calcined at 900°C; e) calcined at 1000°C.

The FTIR spectra of all HA powders are shown in Figure 3. The spectra indicate that the broad peaks at 3400 cm^{-1} (stretching) and 1650 cm^{-1} (bending), which can be assigned to chemically absorbed H_2O , decreased considerably as the calcination temperature was increased. However, the stretching band at 3570 cm^{-1} and the libration band at 630 cm^{-1} originating from OH^- group, as well as the characteristic 600 cm^{-1} band due to the PO_4^{3-} group are still present, regardless of calcination temperature. The persistence of the OH^- group band suggests that the basic apatite structure of the sample is not affected by the calcination, whereas the chemically absorbed water disappeared as the calcination temperature was increased.

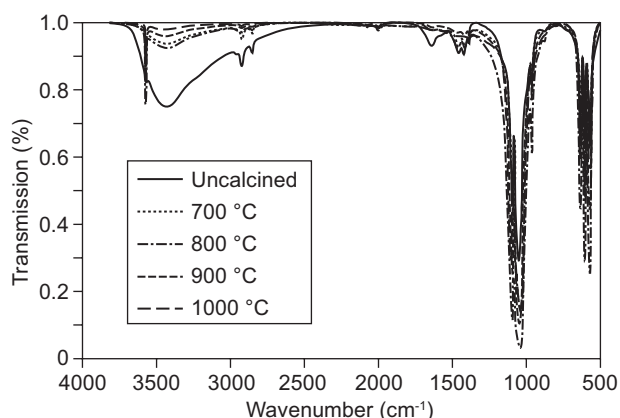


Figure 3. Comparison of FTIR spectra of HA calcined at different temperatures.

Figure 4 shows the X-ray diffractograms of the HA samples sintered at 1350°C. The XRD peaks belong to stoichiometric HA. The results suggest that sintering of the calcined powders did not result in the formation of secondary phases such as tricalcium phosphate (TCP), TTCP or CaO even when sintered at high temperature

of 1350°C. The fact that the calcined HA in the current work did not decompose when sintered at high temperatures is in agreement with the findings of several other authors [19, 21, 22].

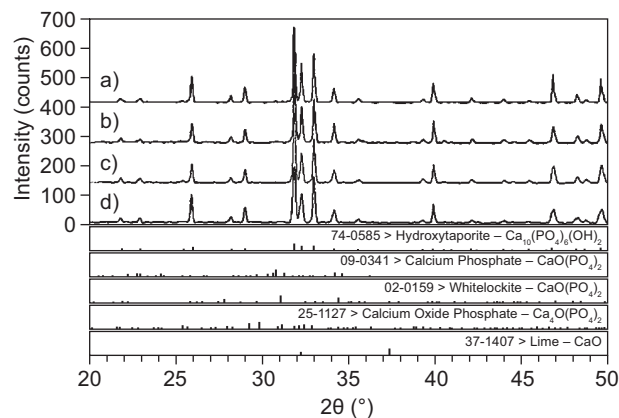


Figure 4. XRD patterns of HA samples sintered at 1350°C, for powders calcined at a) 700°C; b) 800°C; c) 900°C; d) 1000°C.

The densification curves as a function of sintering temperatures are shown in Figure 5. For uncalcined HA samples and samples calcined at low temperatures (< 1000°C), the relative density was high even for lower sintering temperatures. These samples attained relative density > 97 % at a sintering temperature of 1150°C while HA powders calcined at 1000°C could only attain a relative density of ~ 91 % at this temperature. This result showed that calcination at high temperature has some delaying effect on the sintering since higher sintering temperature (1350°C) is needed for this sample to achieve a relative density of ~ 95 %.

The lower sinterability of powder calcined at 1000°C can be attributed to the large agglomerates and fused particles observed in these powders (Figure 1e) prior to compaction and sintering. Özkan and Briscoe [23] have reported that large agglomerates in ceramic powders are often the origin of strength limiting flaws and can affect the densification of the ceramic [24].

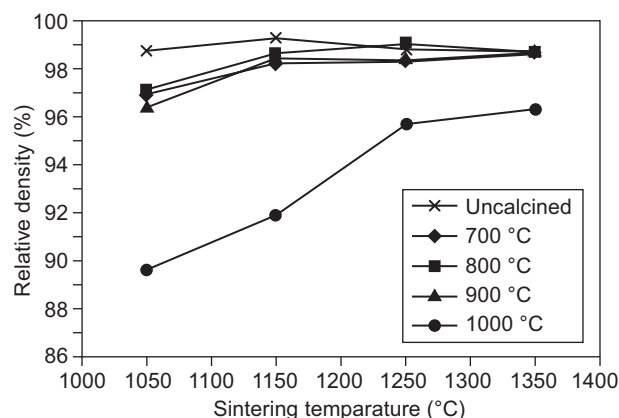


Figure 5. Relative density variation as a function of sintering temperatures for HA.

The variation of the average Vickers hardness for samples sintered at various temperatures is shown in Figure 6. In general, the hardness value of HA material showed no dependence on calcination temperature for powders treated at 700 - 900°C. The hardness, however, decreased with increasing sintering temperature. In the current study, a maximum hardness value of 7.23 GPa was recorded for uncalcined HA when sintered at 1150°C. Calcination at 1000°C prior to sintering proved to be detrimental to the hardness of HA materials. A low hardness value of 1.65 GPa was recorded for this sample when sintered at 1050°C whereas a maximum hardness value of 5.36 GPa could only be attained when samples sintered at 1250°C. For higher sintering temperature (1350°C) the hardness decreased again. The low hardness values of sintered HA materials from HA powder calcined at 1000°C as compared to the uncalcined HA and powder calcined at lower temperatures are obviously related to the low densities of these materials, as shown in Figure 5.

The variation of the average fracture toughness of samples sintered at various temperatures is shown in Figure 7. It is evident that calcination at 700 - 900°C prior to sintering has negligible effect on the fracture

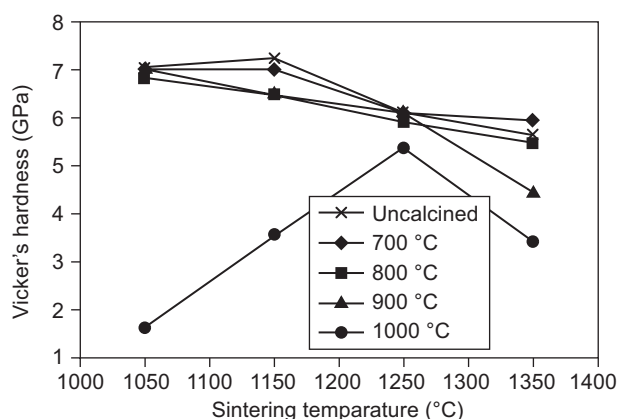


Figure 6. Effect of sintering temperature and calcination temperatures on the Vickers hardness of HA.

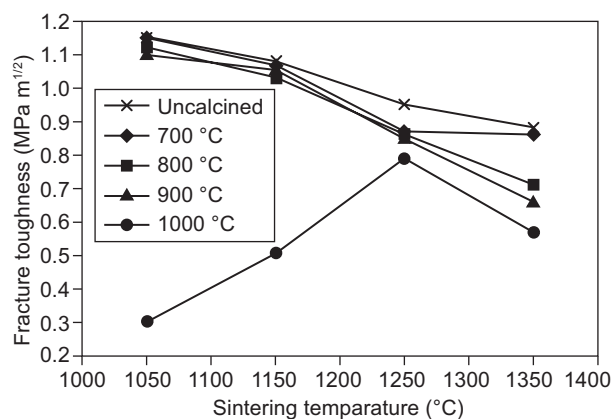


Figure 7. Effect of sintering temperature and calcination temperatures on the fracture toughness of HA.

toughness. The results showed that the fracture toughness of sintered HA materials prepared from HA powders (calcined at temperatures up to 900°C) decreased with increasing sintering temperature, i.e. from a maximum value of $\sim 1.15 \text{ MPa}\cdot\text{m}^{1/2}$ at 1050°C to a minimum value of $\sim 0.88 \text{ MPa}\cdot\text{m}^{1/2}$ when sintered at 1350°C.

CONCLUSIONS

The Ca/P ratio of HA powders prepared by wet chemical processing was not affected by the calcination temperature. XRD confirmed that calcination has no effect on the phase stability of HA (absence of secondary phases such as TCP and CaO). However, the crystallinity of HA powders increased as calcination temperature increased. In addition, it was observed from the FTIR spectrum that the characteristic bands associated to apatitic OH⁻ in the HA matrix were not altered by the calcination temperature. However, the chemically absorbed water gradually disappeared as the calcination temperature was increased to 1000°C. The most significant changes were a sharp decrease in the specific surface area and coarsening of the powders particles as calcination temperature was increased. In terms of sintering behaviour, the study revealed that calcination of HA powder at low temperature (700 to 900°C) prior to sintering has a negligible effect on the sinterability of the HA compacts. However, calcination at 1000°C prior to sintering was found to be detrimental to the properties of sintered HA.

Acknowledgement

The authors gratefully acknowledge PRPUM grant number CG011-2013, UMRG grant number RP024B-13AET, PPP grant number PG080-2013A and FRGS grant number FP046-2013B for the financial support.

REFERENCES

- Hing K.A.: International Journal of Applied Ceramic Technology 2, 184 (2005).
- Muddugangadhar B., Amarnath G.S., Tripathi S., Dikshit S., Divya M.S.: International Journal of Oral Implantology and Clinical Research 2, 13 (2011).
- Chen Q., Zhu C., Thouas G.A.: Progress in Biomaterials 1, 1 (2012).
- Hench L.L.: Journal of American Ceramic Society 81, 1705 (1998).
- Bhardwaj A., Misuriya A., Maroli S., Manjula S., Singh A.K.: Journal of international oral health: JIOH 6, 121 (2014).
- Dorozhkin S.V.: Biomaterials 31, 1465 (2010).
- Ramesh S., Tan C.Y., Sopyan I., Hamdi M., Teng W.D.: Science and Technology of Advanced Materials 8, 124 (2007).

8. Sadat-Shojai M., Khorasani M.T., Dinpanah-Khoshdargi E., Jamshidi A.: *Acta Biomater.* **9**, 7591 (2013).
 9. Adzila S., Sopyan I., Tan C.Y., Ramesh S., Wong Y.H., Purbolaksono J., Hamdi M.: *Indian Journal of Chemistry* **52**, 1570 (2013).
 10. Nasiri-Tabrizi B., Honarmandi P., Ebrahimi-Kahrizsangi R., Honarmandi P.: *Materials Letters* **63**, 543 (2009).
 11. Anitha P., Pandya H.M.: *J. Environ. Nanotechnol.* **3**, 101 (2014).
 12. Rajabi-Zamani A.H., Behnamghader A., Kazemzadeh A.: *Materials Science and Engineering: C* **28**, 1326 (2008).
 13. Jingbing L., Kunwei L., Hao W., Mankang Z., Haiyan X., Hui Y.: *Nanotechnology* **16**, 82 (2005).
 14. Castro F., Kuhn S., Jensen K., Ferreira A., Rocha F., Vicente A., Teixeira J.A.: *Chemical Engineering Science* **100**, 352 (2013).
 15. Patel N., Gibson I.R., Ke S., Best S.M., Bonfield W.: *Journal of Materials Science: Materials in Medicine* **12**, 181 (2001).
 16. Drouet C., Bosc F., Banu M., Largeot C., Combes C., Dechambre G., Estournès C., Raimbeaux G., Rey C.: *Powder Technology* **190**, 118 (2009).
 17. Ramesh S.: *A Method for Manufacturing Hydroxyapatite Bioceramic*, Malaysia Patent no. PI.20043325, 2004.
 18. Niihara K., Morena R., Hasselman D.P.H.: *J. Mater. Sci. Lett.* **1**, 13 (1982).
 19. Juang H.Y., Hon M.H.: *Biomaterials* **17 (21)**, 2059 (1996).
 20. Senamaud N., Bernache-Assollant D., Champion E., Heughebaert M., Rey C.: *Solid State Ionics* **101**, 1357 (1997).
 21. Sadeghian, Heinrich J.G., Moztarzadeh F.: *Ceramics International* **32**, 331 (2006).
 22. Bernache-Assollant D., Ababou A., Champion E., Heughebaert M.: *Journal of the European Ceramic Society* **23**, 229 (2003).
 23. Özkan N., Briscoe B.J.: *Ceramics International* **23**, 521 (1997).
 24. Vishista K., Gnanam F.D.: *Materials Letters* **58**, 1665 (2004).
-